

© Copyright 1991 American Meteorological Society (AMS). Permission to use figures, tables, and brief excerpts from this work in scientific and educational works is hereby granted provided that the source is acknowledged. Any use of material in this work that is determined to be “fair use” under Section 107 of the U.S. Copyright Act or that satisfies the conditions specified in Section 108 of the U.S. Copyright Act (17 USC §108, as revised by P.L. 94-553) does not require the AMS’s permission. Republication, systematic reproduction, posting in electronic form on servers, or other uses of this material, except as exempted by the above statement, requires written permission or a license from the AMS. Additional details are provided in the AMS CopyrightPolicy, available on the AMS Web site located at (<http://www.ametsoc.org/AMS>) or from the AMS at 617-227-2425 or copyright@ametsoc.org.

Permission to place a copy of this work on this server has been provided by the AMS. The AMS does not guarantee that the copy provided here is an accurate copy of the published work.

A HYBRID CARTESIAN WINDFIELD SYNTHESIS TECHNIQUE USING A TRIPLE DOPPLER RADAR NETWORK*

Richard DeLaura and Marilyn M. Wolfson
Lincoln Laboratory, Massachusetts Institute of Technology
Lexington, Massachusetts 02173

Peter S. Ray
Florida State University
Tallahassee, Florida 32306

1. INTRODUCTION

The estimation of air and particle motions in storms from multiple Doppler radar measurements is a long standing problem in radar meteorology. Our research interest in understanding the relationship of electrical charge generation processes above the freezing level to thunderstorm life cycle, and in the detailed quantification of the eventual low altitude divergent outflow produced by the storm, demands an accurate retrieval of air and particle motions at essentially all altitudes within the storm. We found that existing approaches had deficiencies for our needs, and have developed an improved "hybrid" approach which attempts to provide high quality estimates throughout the storm volume.

2. WIND SYNTHESIS TECHNIQUES

For a given radar network geometry, each multiple Doppler wind synthesis technique amplifies the radial velocity and terminal velocity variances differently. Two primary triple Doppler wind synthesis techniques are commonly used: Direct (DIR; Armijo 1969) and Overdetermined Dual (ODD; Ray *et al.* 1980). Most experiments have used widely spaced networks to increase their chances of gathering data on a number of storms (*e.g.*, Kessinger, Ray, and Hane 1987; Table 1). Generally these measurements were made at low elevation angles where ODD wind synthesis techniques give most accurate results, and particle fallspeeds were derived from reflectivity. Only two previous experi-

ments, both in regions with a high frequency of thunderstorms, used closely spaced radar networks (Lhermitte and Williams 1985, and Raymond and Blyth 1989; Table 1). These studies both scanned storms at high elevation angles, and used DIR techniques for wind synthesis and derivation of the vertical particle velocity.

The comparison of wind synthesis techniques, needed for the new "hybrid" approach, may be based on their relative sensitivity of the vertical velocity estimate to errors in the measured radial velocity from each of the radars (*e.g.*, Doviak *et al.*, 1976), and to errors in the particle terminal velocity (V_t). The various techniques are summarized below.

2.1. DIR

DIR resolves the radial velocity wind vectors directly into the Cartesian components u , v , and W ($\equiv w + V_t$). V_t can be estimated from reflectivity data, and the vertical velocity w is then recovered. The equations can be written in an overdetermined, least-squares form for more than 3 radars (Ray and Sangren 1983).

DIR yields estimates of W at high altitudes that are excellent, especially for a network of closely spaced radars. This is illustrated in Fig. 1a, where contours of σ_w are shown at 5 km AGL, assuming $\sigma_v = 1$ m/s for each radar in the

* This work was sponsored by the Federal Aviation Administration. The views expressed are those of the authors and do not reflect the official policy or position of the U.S. Government.

Table 1. Comparison of various wind synthesis techniques used here and in previous multiple Doppler weather radar data analyses (see references for details). Shading in a particular row indicates the technique was used for that radar network. The various wind synthesis techniques are described in section 2. "UP" and "DOWN" refer to the direction of integration of the continuity equation to derive vertical velocity.

AUTHORS:	KESSINGER, RAY & HANE	LHERMITTE & WILLIAMS	RAYMOND & BLYTH	DELAURA, WOLFSON & RAY
DOPPLER WEATHER RADAR NETWORKS: (95 x 65 km maps)				
SYNTHESIS TECHNIQUES	OK	FL	NM	FL
DIRECT	(APPENDIX)		OVERDETERMINED	USED IN HYB & V_t - upper
INT - UP	(APPENDIX)			USED IN V_t - lower
INT - DOWN	(APPENDIX)			USED IN V_t - upper
ODD - UP				USED IN V_t - lower
ODD - DOWN				USED IN HYB
VAR'L ADJUST	ODD - DOWN			USED IN HYB
HYBRID				
$V_t = W - w$				ABOVE & BELOW FRZ. LVL

Orlando network. The contours include the sensitivity of DIR to the accuracy of the terminal velocity estimate (note that $\sigma_w^2 = \sigma_W^2 + \sigma_{V_t}^2$, even though $w = W - V_t$); σ_V is set to 2 m/s. Estimates of W and w at lower altitudes, however, are poor as illustrated by the thin, closely spaced σ_w contours in Fig. 1b at 1 km AGL (σ_w^2 is proportional to $1/z^2$).

2.2. ODD

The ODD method resolves the radial velocity vectors into the horizontal windfield components u and v , and then integrates the mass continuity equation to find the vertical velocity w . When windfield variance estimates are used to quantitatively compare synthesis techniques as they are in our HYB approach, one must be careful to ensure that the estimates are both correct and truly comparable. Previously

published estimates of σ_u^2 and σ_v^2 from ODD omit covariance terms that can contribute significantly to the final result, especially at high altitudes in a closely spaced Doppler radar network. This can be particularly problematic, since σ_u^2 and σ_v^2 also contribute to σ_w^2 through integration of the continuity equation. For ODD, the errors in u and v windfield components are:

$$\sigma_u^2 = \left\{ \frac{1}{[(XX)(YY) - (XY)^2]} \right\}^2 \left\{ T_1 + T_2 + T_3 + T_4 \right\} \quad (1)$$

$$\sigma_v^2 = \left\{ \frac{1}{[(XX)(YY) - (XY)^2]} \right\}^2 \left\{ T_5 + T_6 + T_7 + T_8 \right\}$$

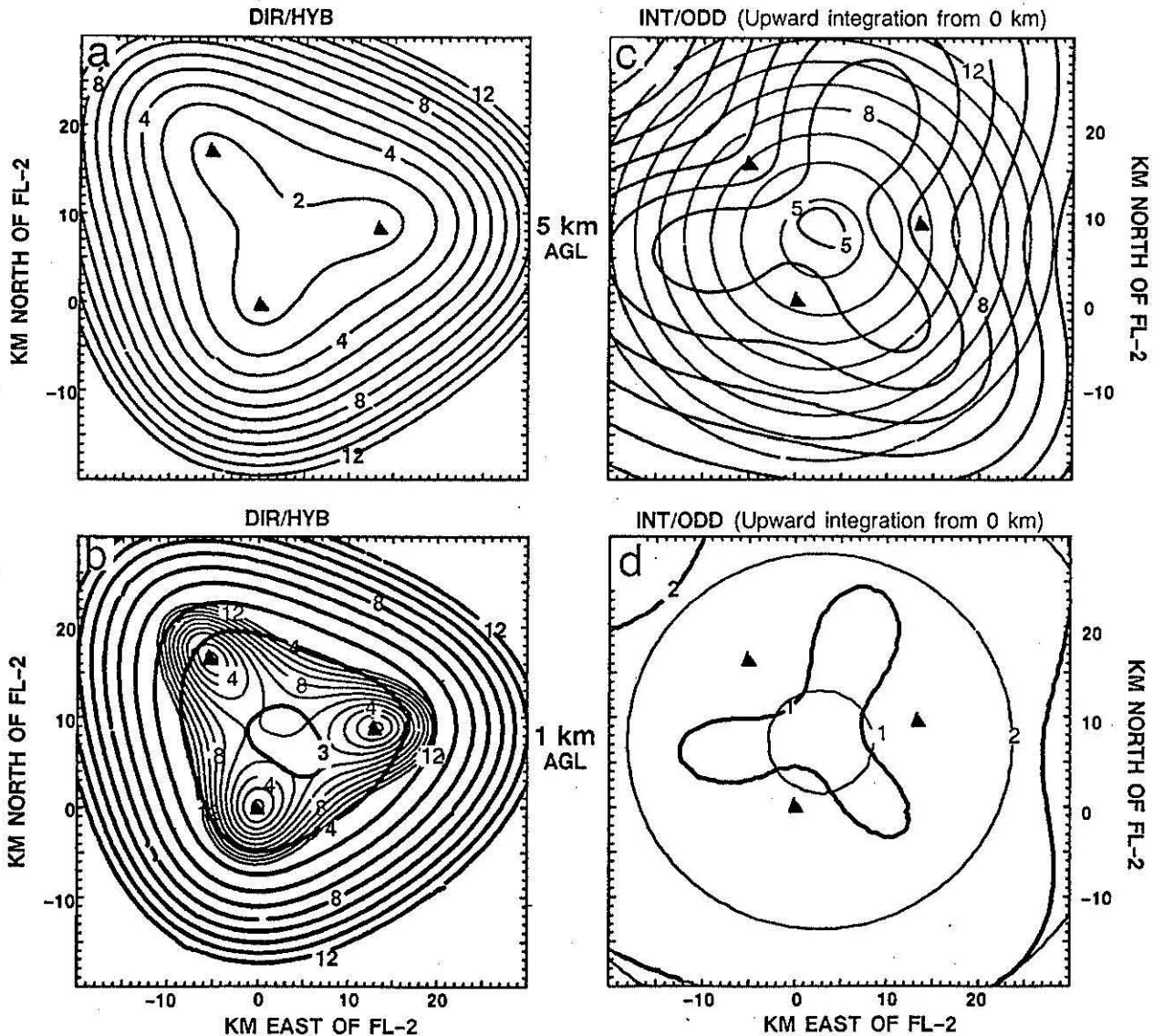


Figure 1. Vertical velocity errors. Comparison of vertical velocity errors (m/s) for DIR/HYB (left column), and INT/ODD (right column). A terminal velocity measurement error of 2 m/s and radial velocity measurement error of 1 m/s were assumed. At left, HYB is shown in the bold contours (note that at 5 km, DIR and HYB are identical). At right, ODD has a lobe pattern and is shown in the bold contours. All fields are contoured at 1 m/s intervals up to 12 m/s. INT and ODD are obtained via upward integration from the ground where $w = 0$. The three black triangles denote the radar network near Orlando shown in Table 1.

where

$$T_1 \equiv (YY)^2 \sum_{i=1}^{i=N} (x-x_i)^2 R_i^2 \sigma_i^2 + (XY)^2 \sum_{i=1}^{i=N} (y-y_i)^2 R_i^2 \sigma_i^2 - 2(XY)(YY) \sum_{i=1}^{i=N} (x-x_i)(y-y_i) R_i^2 \sigma_i^2$$

$$T_2 \equiv 2[(XY)(YY)(YZ) - (YY)^2(XZ)] \sum_{i=1}^{i=N} (x-x_i) R_i \text{cov}(W, V_i)$$

$$T_3 \equiv 2[(XY)(XZ)(YY) - (XY)^2(YZ)] \sum_{i=1}^{i=N} (y-y_i) R_i \text{cov}(W, V_i)$$

$$T_4 \equiv [(XZ)^2(YY)^2 + (XY)^2(YZ)^2 - 2(XY)(XZ)(YY)(YZ)] \sigma_w^2$$

$$T_5 \equiv (XY)^2 \sum_{i=1}^{i=N} (x-x_i)^2 R_i^2 \sigma_i^2 + (XX)^2 \sum_{i=1}^{i=N} (y-y_i)^2 R_i^2 \sigma_i^2 - 2(XY)(XX) \sum_{i=1}^{i=N} (x-x_i)(y-y_i) R_i^2 \sigma_i^2$$

$$T_6 \equiv 2[(XX)(XY)(YZ) - (XY)^2(XZ)] \sum_{i=1}^{i=N} (x-x_i) R_i \text{cov}(W, V_i)$$

$$T_7 \equiv 2[(XX)(XY)(XZ) - (XX)^2(YZ)] \sum_{i=1}^{i=N} (y-y_i) R_i \text{cov}(W, V_i)$$

$$T_8 \equiv [(XY)^2(XZ)^2 + (XX)^2(YZ)^2 - 2(XY)(XZ)(YY)(YZ)] \sigma_w^2$$

and where

x_i, y_i, z_i = coordinates of the i^{th} radar

$$R_i = [(x-x_i)^2 + (y-y_i)^2 + (z-z_i)^2]^{0.5}$$

$$(XX) \equiv \sum_{i=1}^{i=N} (x-x_i)(x-x_i) \text{ etc., and}$$

V_i = radial velocity from i^{th} radar.

Eqs. (1) each contain two terms that include the covariance of W with V_i , [$\text{cov}(W, V_i)$]. The exact evaluation of $\text{cov}(W, V_i)$ is hardly straightforward, but one may arrive at a reasonable estimate by considering the relationship between W and V_i for a single Doppler radar:

$$W = V_i \frac{(z-z_i)}{R_i}; \quad \Delta W = \Delta V_i \frac{(z-z_i)}{R_i}; \quad \Delta W \Delta V_i = \Delta V_i^2 \frac{(z-z_i)}{R_i};$$

$$\text{cov}(W, V_i) = \sigma_{V_i}^2 \frac{(z-z_i)}{R_i} \quad (2)$$

This estimate of $\text{cov}(W, V_i)$ is only approximate for ODD, since W and V_i are not actually related by Eq. (2). However, since ODD seeks to find a value of W that minimizes the error in Eq. (2) for all radars in the network, this estimate may be reasonable. The magnitude of the commonly omitted terms is proportional to z^2 , where z is height, because the coefficient multiplying the covariance also includes a linear z dependence. These terms significantly reduce the ODD σ_w^2 at high altitudes. Figure 2 illustrates the difference in the ODD vertical velocity error resulting from the inclusion of terms involving $\text{cov}(W, V_i)$.

2.3. INT

An alternative technique is to use u and v from DIR in the mass continuity equation which can be integrated to find w , eliminating the need for a $V_i - Z$ model. This method we abbreviate as INT for "integrated direct". As in ODD, either a top or bottom boundary condition on w is needed to start the integration.

INT (and DIR) yield consistently good results for u and v throughout the grid (σ_u^2 and σ_v^2 are virtually indepen-

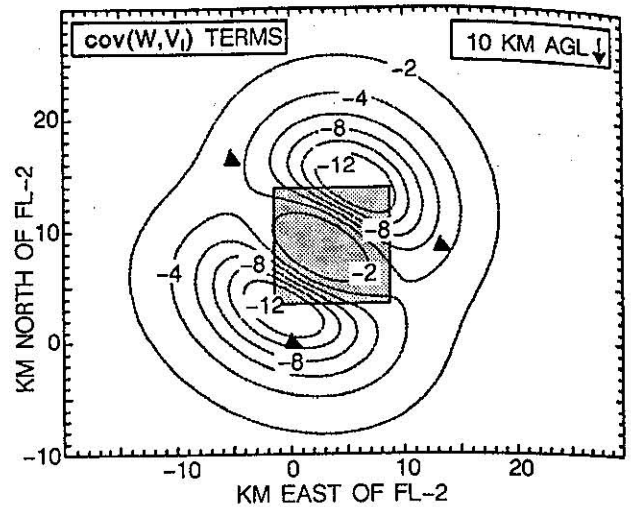


Figure 2. Contours of vertical velocity error differences (m/s) between the ODD technique including $\text{cov}(W, V_i)$ terms, and the ODD technique omitting those terms, are shown at 10 km AGL, for downward integration from 16 km (where $\sigma_w = 0$ m/s was assumed). Contours are drawn every 2 m/s from -12 m/s. Grid spacing is 1 km. The three black triangles denote the radar network near Orlando shown in Table 1. The stippled box is the area in which synthesis techniques are compared later in section 3.

dent of altitude; the only dependence is implicitly contained in R_i), but ODD yields poor estimates of u and v at high elevation angles. Even when the covariance is included, these poor u and v estimates unacceptably contaminate w . ODD with upward integration of the continuity equation (1) yields good results at low altitudes (a flat terrain allows a very accurate $w=0$ boundary condition to be specified). Results from INT are almost as good, but the area of low σ_w is smaller, as illustrated in Figs. 1c and 1d where the circular patterns reflect σ_w achieved with INT and the lobe patterns reflect σ_w achieved with ODD. The problem is that errors in w accumulate quite rapidly with upward integration. Downward integration of the continuity equation (1) produces less accumulated error due to the gradient in atmospheric density (Ray *et al.* 1980), but it requires an accurate estimate of w at the top boundary of the grid which may be impossible to obtain. Vertical velocity estimates from ODD show a weak implicit dependence on V_i while estimates from INT show none.

2.4. HYB

HYB overcomes the disadvantages of the other techniques by applying them only where they are most accurate. The use of DIR at high altitudes supplies an accurate upper boundary condition on w with known variance for the synthesis of windfields at lower altitudes via ODD with downward integration. The basic HYB procedure is given below.

1. Cartesian windfields are calculated using DIR at z_n , the top altitude in the grid.
2. w and σ_w^2 are calculated at the boundary $z_{n-1/2}$, using DIR.
3. σ_w^2 is calculated at the next altitude in the Cartesian volume grid z_{n-1} for both techniques. ODD variances are calculated using σ_w^2 at $z_{n-1/2}$ as the boundary value.
4. σ_w^2 is compared at each point of interest at the current grid level, and the technique whose error is smaller a

the greater number of points is used to calculate u , v , w , and W at z_{n-1} .

- If DIR is deemed more accurate, the steps are repeated for the next grid altitude z_{n-2} , and so on. If ODD is deemed more accurate, u , v and w are calculated at z_{n-1} and $z_{n-3/2}$ using the boundary values calculated at $z_{n-1/2}$ by DIR. Once ODD is deemed more accurate, it is used to calculate windfields throughout the remainder of the grid.
- Estimates of u , v , and w may be refined by setting $w=0$ at the ground, and variationally adjusting the windfield estimates throughout the grid (Ray *et al.* 1980).

The comparison of variance in step 4 may be refined to include variance magnitude weighting or horizontal variances. The comparison may also be restricted to the subset of grid points that fall within a user-defined region (the technique used here) or regions of high reflectivity (*e.g.*, the central region of the storm). The choice of "better" remains somewhat subjective, even when the numeric criterion of variance has been defined.

Finally, since INT windfield estimates are independent of V_i , they may be used in conjunction with HYB to provide estimates of V_i . At lower altitudes, where both ODD \uparrow and INT \uparrow are reasonably accurate, INT estimates for u or v , and w ($= W - V_i$) may be substituted into the ODD equations to yield V_i . At higher altitudes, V_i may be found by taking the difference between the DIR estimate of W and the INT \downarrow estimate of w , provided that an accurate upper boundary value for integrating w may be determined. Another approach would be to derive a $V_i - Z$ relationship from the V_i estimates made only where (DIR and INT \downarrow) and (ODD \uparrow and INT \uparrow) are most accurate (high altitude and low altitude, respectively), and use these to define the $V_i - Z$ models for HYB above and below the freezing level. These models could be updated for each storm analysis volume.

In the example shown in Fig. 1, the HYB switch altitude from DIR to ODD occurred at 3 km AGL. Examination of the bold contours of σ_w for the HYB technique in Fig. 1b shows much lower errors than for DIR at 1 km, and an error pattern that is a combination of the DIR pattern in Fig. 1a and the ODD pattern in Fig. 1d. A variational adjustment of the HYB windfield with $w=0$ at the ground can reduce the HYB σ_w errors even further.

3. APPLICATION TO MODEL DATA

The ODD, DIR, INT and HYB synthesis techniques were tested using a model "true" windfield of a mature Florida thunderstorm supplied by John Anderson at the University of Wisconsin. The model provided reflectivity, temperature, and air velocity ($V_i=0$) data at each point in a 25 x 25 x 19 km grid, with 500 m spacing. Figure 2 shows the locations of the Doppler radar network (triangles) and the error comparison region used in HYB (stippled box).

The model winds were transformed directly into radial Doppler velocities at each point in the grid, then rounded to the nearest integer to simulate measurement errors. Profiles of the *rms* wind synthesis errors in vertical velocity over the error comparison region are shown in Fig. 3. HYB retains the advantages of DIR without the large error at low altitudes. A variational adjustment would reduce the HYB errors even more in the lowest layers, to equal the ODD error at the bottom boundary.

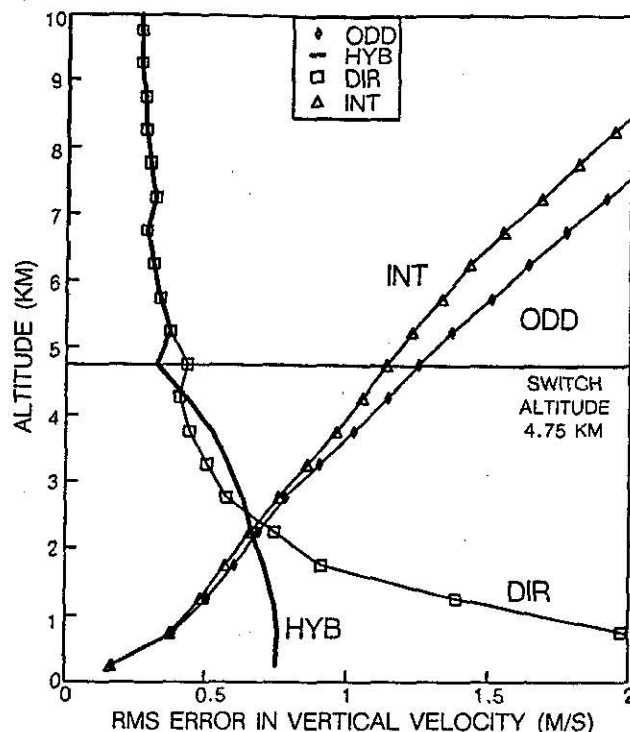


Figure 3. RMS error in vertical velocity for the four wind synthesis techniques as a function of altitude, over the central part of the grid shaded in Fig. 2. The true windfield was a microburst model windfield supplied by Anderson, U. Wisconsin.

4. CONCLUSIONS

The hybrid (HYB) wind synthesis technique combines triple Doppler wind synthesis techniques accurate at high altitudes with techniques accurate at low altitudes in a single storm analysis. It uses the vertical velocity error estimates to select the better windfield synthesis technique at each altitude in the grid, and overcomes the need to specify assumed boundary conditions or $V_i - Z$ models. HYB represents an improvement over ODD and DIR techniques when accurate air and particle motions are required at all altitudes in a storm.

ACKNOWLEDGEMENTS

We thank Barbara Forman and Margo Liepins for their gracious assistance with some of the calculations, and Prof. John Anderson, University of Wisconsin, for the numerical model data.

REFERENCES

- Armijo, L., 1969: A theory for the determination of wind and precipitation velocities with Doppler radars. *J. Atmos. Sci.*, **26**, 570-573.
- Doviak, R.J., P.S. Ray, R.G. Strauch, and L.J. Miller, 1976: Error estimation in wind fields derived from dual-Doppler radar measurement. *J. Appl. Meteor.*, **15**, 868-878.
- Kessinger, C.J., P.S. Ray, and C.E. Hane, 1987: The Oklahoma Squall Line of 19 May 1977. Part I: A multiple Doppler analysis of convective and stratiform structure. *J. Atmos. Sci.*, **44**, 2840-2860.
- Lhermitte, R. and E. Williams, 1985: Thunderstorm electrification: A case study. *J. Geophys. Res.*, **90**, 6071-6078.
- Ray, P.S., C.L. Ziegler, W. C. Bumgarner, and R. J. Serafin, 1980: Single- and multiple-Doppler radar observations of tornadic storms. *Mon. Wea. Rev.*, **108**, 1607-1625.
- Ray, P.S. and K. L. Sangren, 1983: Multiple-Doppler radar network design. *J. Climate Appl. Meteor.*, **22**, 1444-1454.
- Raymond, D. J. and A. M. Blyth 1989: Precipitation development in a New Mexico thunderstorm. *Quart. J. Roy. Meteor. Soc.*, **115**, 1397-1423.